Journal of
Clinical & Cellular Immunology

Barden et al., J Clin Cell Immunol 2016, 7:3
http://dx.doi.org/10.4172/2155-9899.1000432

Research Article Open Access

Therapeutic Targeting of the Cancer-Specific Cell Surface Biomarker nfP2X$_7$

Julian A Barden[1*], Angus Gidley-Baird[1], Liew Cheng Teh[1], G-Halli Rajasekariah[1], John Pedersen[2], Neil I Christensen[3], Derek Spielman[4] and David M Ashley[5]

[1]Biosceptre (Aust) Pty Ltd, Riverside Life Sciences, 11 Julius Ave, North Ryde, N.S.W. 2113, Australia
[2]TissuPath, 165 Burwood Rd, Hawthorn, Vic 3122, Australia
[3]School of Veterinary Medicine, University of Wisconsin, Madison, WI 53706, USA
[4]Department of Veterinary Pathology, the University of Sydney, N.S.W. 2006, Australia
[5]Deakin University, School of Medicine, Geelong, Vic. 3217, Australia

Abstract

The degree of unmet need for new therapeutics in oncology is clear since about 30% of the population die from cancer with enormous associated costs in health care and in personal impact. New and preferably specific targets are needed now to address the problem, both to improve overall survival and importantly to reduce side effects in order to improve quality of life. nfP2X$_7$ is a receptor that, unlike P2X$_7$, cannot enable apoptosis in cancer cells. Having established the widespread coverage of human cancers in which the aberrant receptor is found, attention has been drawn to the therapeutic potential of the target and whether an immunotherapeutic approach is capable of providing a significant therapeutic response. We demonstrate the intrinsic target specificity, the delivery of antibody within target cells, the extremely good safety profile of the targeting antibody and the broad range of cancer tissue that could be treated in both humans and other animals.

Keywords: nfP2X7 receptor; Oncology; Immunotherapy; Antibody; Cancer; Immunohistology

Introduction

P2X receptors form ATP-gated cation-selective channels on the plasma membrane of cells in a range of tissues such as smooth muscle and nerves [1-4]. P2X$_7$ is one such member of this ionotropic purinergic receptor family. The P2X$_7$ subtype mediates cell death, particularly in haematopoietic and immune cells including thymocytes [5], dendritic cells [6], lymphocytes [7,8], macrophages [9] and monocytes [10] and is critically important for phagocytosis [11-13]. The receptor is also present in other cell lineages at some stage of the cell cycle. These include epithelial, mesenchymal and neural cell types [14-17]. P2X receptors exhibit two homologous transmembrane domains separating a similar sized extracellular domain from intracellular domains of variable size. These transmembrane segments show the most homology across P2X subtypes. P2X$_7$ has a short N-terminal intracellular segment and, unlike other P2X subtypes, a long intracellular C-terminal domain [18]. The C-terminal domain is critical for supplying the measured pore-forming properties of the homotrimeric membrane channel [19-20]. Prolonged exposure of the assembled channel to ATP in which all three sites are occupied close to the neighbouring residues K193 and K311 juxtaposed from adjacent monomers, found critical for function [21], results in additional pore dilation [20,22,23]. Saturation ATP binding to the three binding sites formed by the correct packing of the monomers in the trimer results in a rapid increase in the influx of calcium that results in turn in the activation of caspases [24], leading to apoptosis of the affected cell [25].

However, the P2X$_7$ receptors expressed on the surface of the cancer cells are unable to induce apoptosis [26,27]. These receptors continue to function as calcium channels due to the continued integrity of one of the ATP binding sites but lack the ability to form dilated pores [28]. They are identified as non-functional for pore formation and called nfP2X$_7$ [27]. Since the receptors have ATP binding sites formed only by the correct packing of the monomers, the residual calcium current induced by ATP binding suggests that at least two of the monomers are correctly packed in order to form a single ATP binding site. A single incorrectly packed monomer could therefore disrupt two of the ATP binding sites [27]. The disruption at these sites would prevent pore formation and consequent apoptosis. Incorrect packing of a monomer in the trimer may arise from a minor disruption in interactions with one or more of the eleven intracellular accessory binding proteins needed to anchor P2X$_7$ in the plasma membrane. Alternative mechanisms for disruption of the ATP binding sites may involve the insertion of a splice isoform or monomer with a single nucleotide polymorphism into the P2X$_7$ trimer [29,30]. Irrespective of the mechanism or mechanisms giving rise to the exposure of epitopes such as part of 200-216 in the pair of ATP binding domains that become exposed in nfP2X$_7$ conformers, a pair of selective targets is presented that is unavailable on P2X$_7$ [26,27]. Selective targeting of an otherwise hidden pair of epitopes on the receptor surface allows for exquisite discrimination between any normal cells that may express fully functional P2X$_7$ and transformed cells that express non-functional receptors.

Most normal human tissues including skin [14], breast [15] and prostate [16] appear largely devoid of P2X$_7$ receptors until the onset of cancer [27]. Cancer tissues from a wide range of human and other animal sources demonstrate significant levels of surface nfP2X$_7$ receptor expression [27]. The nfP2X$_7$ membrane current drives proliferation [28] and morphological change through shedding of anchorage proteins leading to cells showing the highest aberrant nfP2X$_7$ receptor-induced current becoming the cells with the highest invasion potential [27].

While surface residues on the P2X$_7$ protein vary widely between species, the small and specific target epitope exposed in nfP2X$_7$ is highly conserved. Thus, antibodies designed to detect nfP2X$_7$ in human tissue have the potential to detect any such aberrant receptor in other species. The binding constant of ATP for P2X$_7$ is relatively high, 0.1 mM

***Corresponding author:** Julian A Barden, Biosceptre (Aust) Pty Ltd, Riverside Life Sciences, 11 Julius Ave, North Ryde, N.S.W. 2113, Australia, Tel: 124908280 ; E-mail: julian.barden@biosceptre.com

Received: May 27, 2016; **Accepted:** June 13, 2016; **Published:** June 21, 2016

Citation: Barden JA, Gidley-Baird A, Teh LC, Rajasekariah GH, Pedersen J, et al. (2016) Therapeutic Targeting of the Cancer-Specific Cell Surface Biomarker nfP2X$_7$. J Clin Cell Immunol 7: 432. doi:10.4172/2155-9899.1000432

[26]. A slight variant fold at the monomer-monomer interfaces that is assembled between the single incorrectly folded or packed monomer and the pair of adjacent correctly packed monomers would result in loss of ATP binding at these two altered sites. Any mutation in these critical residues is likely to disrupt ATP binding. ATP would either bind more weakly, and therefore effectively not at all, resulting in loss of function or else would bind more strongly, leading to an accidental prolonged receptor activation resulting in unwanted cell death. The absence of mutations in the critical epitope underlying the ATP binding site across species is singularly indicative of its importance to receptor structure-function [27]. Antibodies to such a conserved target in humans, exposed only when cells are attempting to initiate apoptosis, could therefore be used to test for both safety and efficacy in a wide range of species used in the drug development process, greatly reducing risks from off-target side effects. The presence of a high density of fully functional P2X$_7$ receptors on leukocytes makes specific targeting of this receptor especially important in order to avoid neutropaenia.

Here we examine the specific binding of affinity purified polyclonal antibodies to cancer tissue and the therapeutic potential of the nfP2X$_7$ target.

Methods

Specimens

Prostate biopsy tissues and the marsupial Tasmanian Devil tumour tissue samples and cat tissue samples were supplied from the laboratories of contributing authors JP, DS and NC, respectively.

Tissue labelling

Biopsy tissues were processed in order to carefully ensure thorough, but not over fixation, with standard paraffin embedding. Paraffin sections were cut to approximately 5 μm and placed on coated slides that were usually stained within 2-3 days of being prepared as described [27].

Antibody preparation

Sheep were immunised against the nfP2X$_7$ target epitope 200-216 [26]. Target specific IgG antibody was affinity purified on an Affigel-10 column with elution controlled by an Akta Explorer. The antibody was labelled with FITC (Pierce 50327) for direct microscopy.

Cell preparation

PC3, COLO205, 4T1, B16 and HEK293 cells were supplied by ATCC. PC3, COLO205 and 4T1 cells were cultured in standard RPMI complete medium. A 500 mL bottle of RPMI-1640 (GibcoBRL 11875-093) had the following constituents added; 5.0 mL 1 M HEPES (pH 7.0), 5.0 mL Sodium Pyruvate (100 mM, Sigma S-8636), 5.0 mL Penicillin (10,000 U)-Streptomycin (10 mg)-L-Glutamine (200 mM) solution (Sigma G-1146), 0.5 mL 2-Mercaptoethanol solution (50 mM), 50 mL heat inactivated (40 min at 56°C) Foetal Calf Serum (HyClone SH30070.03. Cells were grown to 70% confluence and detached using Cell Dissociation Buffer (Life Technologies 13151-014) to avoid trypsinisation that may influence the target receptors. The cells were washed once with RPMI and reseeded in a new flask. B16 cells were cultured in DMEM (Gibco) with FCS. The human D270 glioma cells were obtained from Royal Melbourne Children's Hospital [30].

Cell killing assay

The Promega Cell Titer Blue assay kit (G8081) was used to determine the effects of the antibody on growth inhibition and cell death. D270 cells were seeded into wells on a 96-well plate (Primaria) and incubated with 15 uM cisplatin (Royal Melbourne Children's Hospital) in the presence of an increasing concentration of specific sheep antibody. Cells were analysed on Day 4.

HEK293 transfection

Cells were maintained in DMEM and viability exceeding 90% established prior to transfection. DNA corresponding to the extracellular domain of the receptor was diluted in Lipofectamine (Life Technologies) Reagent using Opti-MEM Reduced Serum Medium (31985-070).

Flow cytometry

Cells were grown to 70-90% confluency in T75 flasks. The supernatant was aspirated and the cells washed twice with buffer and aspirated. Cell dissociation buffer (2 mL) was added for 20 min at 37°C and the cells dislodged by gentle tapping of the flask. Primary or secondary antibodies were aliquoted into the flow tubes in readiness for the addition of the cells. Cells were resuspended and pooled in a 50 mL Falcon tube with buffer added to 50 mL. Cells were centrifuged at 500 x g at 25°C and supernatant discarded and the process repeated. Cells were counted using haemocytometer. Cell pellet was resuspended in HBSS (Gibco 21250-022) with 2% FCS to 1.5×10^6 cells/mL. Each flow run on the Beckman Coulter Quanta SC used up to 100 uL of cell suspension. Specific and control antibodies were added to appropriate tubes and cells incubated for 20 min at 4°C. The secondary antibody (Southern Biotech SB601002 rabbit F(ab)$_2$ anti-sheep IgG(H+L)-FITC) was used at 1:25 for 20 min. at 4°C in the dark. The cells were washed with 1 x HBSS and 2% FCS, the cells were centrifuged at 200 x g for 5 min at 4°C and supernatant aspirated prior to pellet resuspension in the same buffer to which was added 1 uL of 7AAD (Beckman Coulter IM3422) in order to identify dead cells so these could be excluded from analysis.

Results

Species cross-reactivity

The appearance of novel and ubiquitous nfP2X$_7$ receptors at the onset of human and other mammalian cancers indicates that the antibody probe can be used as an important adjunct to current diagnoses of cancer. Evidence for the broad appearance of nfP2X$_7$ in human cancers has been shown [27]. The reagent developed for the formalin fixed and paraffin embedded (FFPE) human tissue sections can be used to detect receptor expression in tumour sections from other species. An example of a tumour arising in a non-human is shown in the form of sections from the Tasmanian Devil, a marsupial that is suffering from Devil Facial Tumour Disease (DFTD) transmitted between animals as a result of transfer of a small number of clonal cancer cells from bites when fighting. A section of the primary was stained for nfP2X$_7$. The edge of the tumour on the skin surface is shown in Figure 1a. Figure 1b reveals a clear cytoplasmic and membranous distribution on affected cells supported by normal stroma in the deeper transformed zone of the primary tumour. Metastatic cells appear in the lung. These too are clearly stained for nfP2X$_7$ (Figure 1c). Similar patterns are seen in mice, possums and domestic animals such as cats and dogs.

Increase in nfP2X$_7$ receptor expression with tumour grade

There are indications that the nfP2X$_7$ receptor expression varies with tumour grade, at least in prostate cancer, providing the potential to differentiate between latent and aggressive forms of cancer. Tissue biopsies taken from men with confirmed cancers graded for Gleason score or confirmed normal by repeat negative biopsies over time were stained for nfP2X$_7$ receptor. Sections of FFPE tissue taken from patients

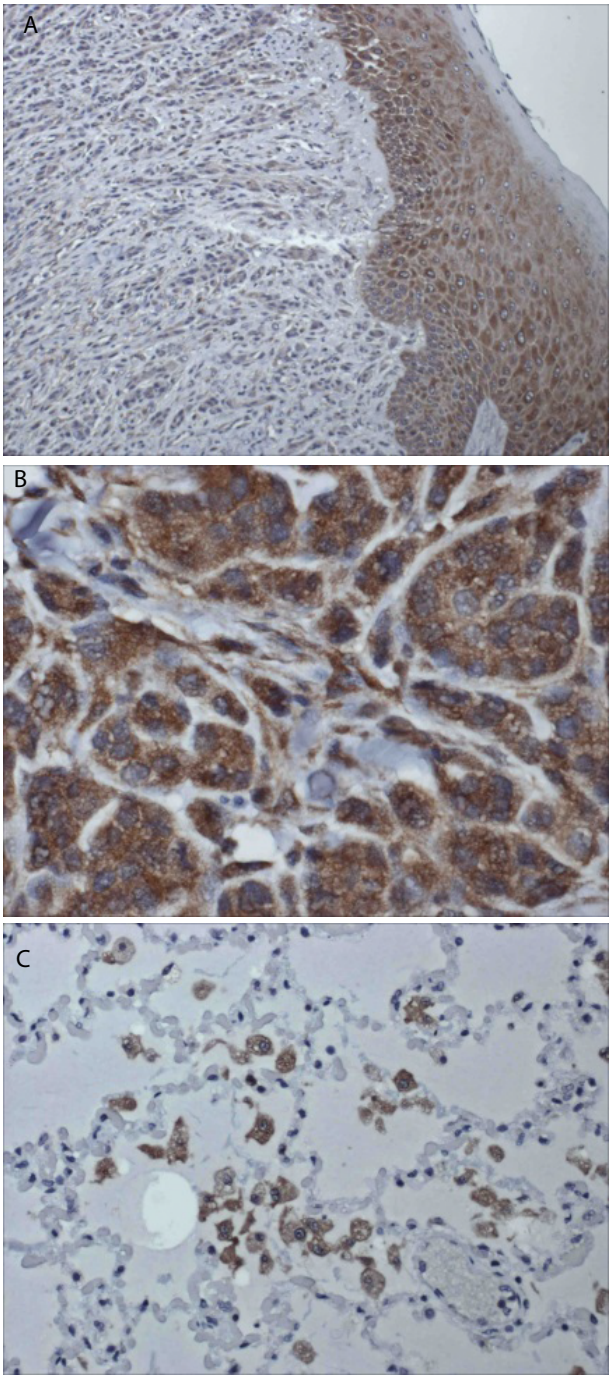

Figure 1: Sections of the marsupial Tasmanian Devil facial tumour disease (DFTD) **(A)** primary tumour on edge of skin (10x obj); and **(B)** primary tumour in deeper transformed zone (10x obj); and **(C)** lung secondary (40x obj) show clear evidence for the presence of the nfP2X$_7$ receptors.

confirmed as normal were devoid of stain for the receptor (Figure 2a). In patients who were found to have small low grade tumours, areas of normal morphology in adjacent regions showed weak cytoplasmic stain in the apical epithelium (Figures 2b and 2c). Larger confirmed tumours that still remained well differentiated (Gleason Grade 6) more generally exhibited much heavier stain in the apical epithelium in areas of normal histology adjacent to the tumour (Figure 2d). The stain appearing on sections of still normal morphology adjacent to higher grade tumours i.e. those tumours that had transformed from being well-differentiated to moderately or poorly differentiated was more likely to be stronger and showed a characteristic pattern in which the basement membrane became heavily stained (Figure 2e). This pattern appeared prior to stromal invasion in the stained sections. The pattern was continued in the tumour sections (Figure 2f) in which stromal invasion was apparent and often where higher grade tumour had appeared in the apical epithelium. Stromal stain was a strong feature and indicative of shed receptor displaced from the adjacent affected apical epithelium as such stain was absent further from the tumour centre.

In vitro binding to live cells

Affinity purified sheep anti-nfP2X$_7$ antibody was tested for specific binding to the target conformational epitope by generating the P2X$_7$ extracellular domain (ECD) recombinantly and by transfecting it into HEK293 cells. Flow cytometry was used to measure binding to mock transfected (no DNA), empty transfected (no P2X$_7$ DNA) and those transfected with the extracellular domain monomers. Dose-dependent specific binding of the sheep anti-nfP2X$_7$ IgG antibody to the ECD on the cell surface was measured over the concentration range 4-128 nM (0.6-20 μg/mL). Binding to either mock or blank vector transfected cells was less than 2%, similar to the level recorded for secondary antibody conjugate alone (Figure 3).

Specific binding to nfP2X$_7$ receptors was examined on a wide range of cancer cell types using flow cytometry. An example is shown using live COLO205 cells in Figure 4. The results of these studies using FITC-labelled sheep anti-nfP2X$_7$ indicated strong binding. Reproducible strong binding of the sheep anti-nfP2X$_7$ IgG to live tumour cells known to express nfP2X$_7$ from immunohistochemical studies on tumour cells in cytospins and fixed cancer tissue sections suggested the potential utility of the antibody for targeted killing of tumour cells, provided there was little or no cross-reactivity with P2X$_7$ expressed on normal cells such as lymphocytes. Human B-lymphocytes were extracted from donor blood and the same sheep antibodies tested for binding. There was no detectable shift in the mean fluorescence intensity with either control or specific anti-nfP2X$_7$ antibody above the signal detected for samples containing cells only thus indicating no cross-reactivity with wild type functional receptor.

Endocytosis of sheep anti-nfP2X$_7$ antibody in PC3 cells

PC3 cells were grown on coverslips and preincubated on ice with 100 nM FITC conjugated affinity purified sheep anti-nfP2X$_7$ IgG antibody for 30 minutes and then washed with PBS. Coverslips were fixed immediately (Figure 5a) or incubated in normal media at 37°C for 30 minutes (Figure 5b) or 2 hours (Figure 5c) before fixation. Cells were counterstained with Hoescht and imaged by confocal microscopy. After preincubation (Figure 5a) only surface binding of sheep anti-nfP2X$_7$ is seen, upon incubation at 37°C antibody rapidly internalises after 30 minutes (Figure 5b) and accumulates in intracellular compartments after 2 hours (Figure 5c).

In vitro tumour cell killing

Studies were undertaken to observe direct cell killing effects of the affinity purified sheep anti-nfP2X$_7$ IgG antibody either alone or in combination with standard cytotoxic drugs.

Human D270 malignant glioma cells are resistant to low levels of cisplatin. These were tested to determine whether there was augmented cell killing in the presence of the sheep anti-P2X$_7$ IgG antibody. Cells were

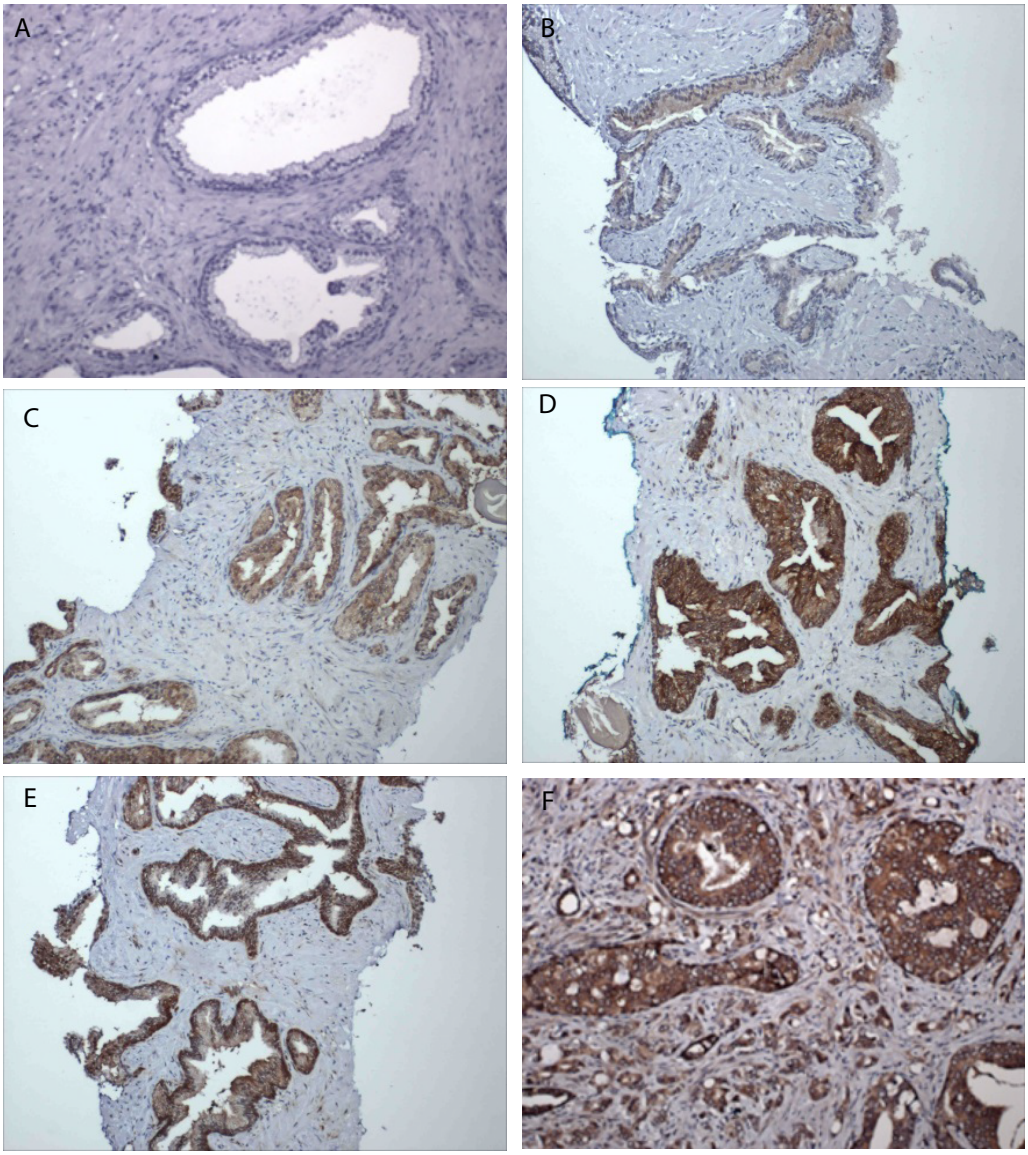

Figure 2: A series of biopsies from prostate tissue from men suspected of harbouring prostate cancer. The confirmed absence of cancer based on multiple repeat biopsies over time is associated with a lack of expressed nfP2X$_7$ **(A)**. The presence of small low-grade tumours is associated with a weak cytoplasmic distribution ranging from just detectable in benign adjacent areas **(B)** to a stronger cytoplasmic expression **(C)**. A larger tumour but generally still confined to well-differentiated Gleason Grade 6 shows a much heavier receptor density in the apical epithelial cells in the areas of normal morphology adjacent to the identified tumour, again with majority cytoplasmic expression **(D)**. Tumour transformation to Gleason Grade 7 and above where the tumour has become moderately differentiated shows the characteristic expression of receptors on the basement membrane in anticipation of the ensuing stromal invasion **(E)**. An example of the moderately and poorly differentiated later stage tumours that give rise to the basement membrane receptor stain pattern in adjacent morphologically normal-appearing tissue such as **(E)** is shown in section **(F)** where widespread stromal invasion is apparent and there is evidence of Gleason Grade 9/10 in the acini.

incubated at 37 °C in the presence of a 15 uM sub-lethal concentration of cisplatin and sheep anti-nfP2X$_7$ IgG antibody in concentrations ranging up to 24 nM for 24 h. Control wells were treated with the same concentrations of control sheep IgG and cell death measured by Cell Titer Blue assay. The background percentage of dead cells in the control wells was 15%. Specific antibody concentrations above 6 nM resulted in increased cell death (Figure 6). At 24 nM the specific antibody increased cell killing to 47% compared with 23% with the control, a concentration that is readily attainable in serum by intravenous injection.

In vivo efficacy in mouse xenograft tumour models

A model of the inhibition of growth and spread of metastases was established in Balb/C mice inoculated with the 4T1 breast tumour cells. Groups of 8 mice were randomly assigned after inoculation into those treated with control buffer injections and those treated with the sheep anti-nfP2X$_7$ IgG antibody at 10 mg/kg in 2 mM citrate buffer. Injections via tail vein occurred on Days 0, 2, 4, 6, 9 and 12. Animals were sacrificed on Day 14 and the tissues examined for lung metastases. The results are shown in Figure 7. An average of 8.1 metastases were present in the control mice while there was an average of only 3.1 per mouse in the treatment group. Results were significant at $P<0.001$ with t-test.

The aggressive B16 intradermal mouse melanoma model was

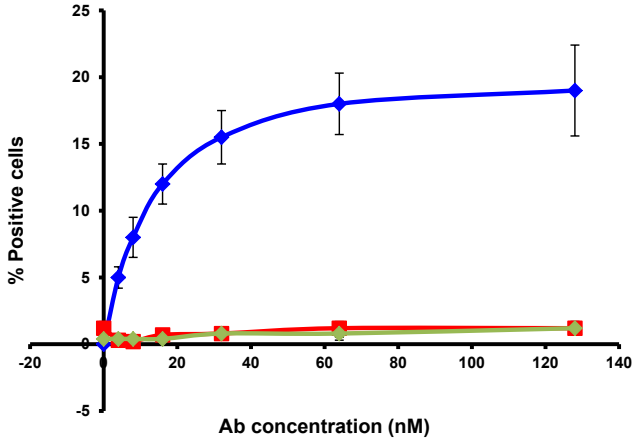

Figure 3: Flow cytometry measurement (mean ± SEM) of affinity purified sheep anti-nfP2X$_7$ IgG antibody binding to the extracellular domain of human P2X$_7$ transfected in HEK293 cells. Cells were transfected with ECD (blue), mock (red) and empty vector (green).

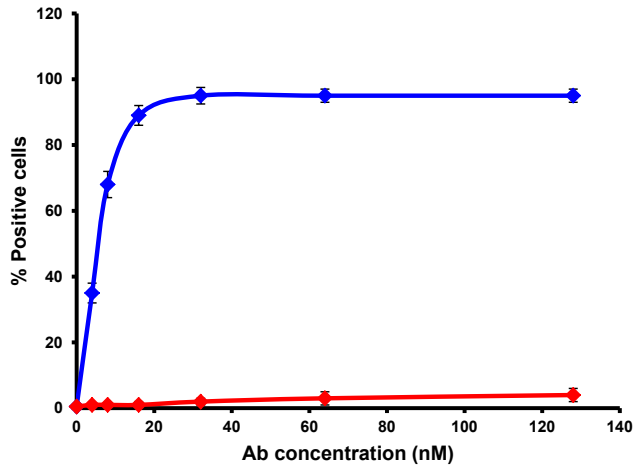

Figure 4: Flow cytometry measurement (mean ± SEM) of affinity purified sheep anti-nfP2X$_7$ IgG antibody binding to the human colorectal tumour cells COLO205 (blue) compared with low background binding of the FITC-labelled control sheep IgG antibody (red). The background signal is similar to the low levels of the control antibody.

used to measure the effect of a topical application of sheep anti-nfP2X$_7$ antibody or non-specific control sheep IgG on *in vivo* tumour growth inhibition. In this study female black hairless C57/BL6 mice were injected intradermally with B16 melanoma cells and randomly allocated to groups that were untreated controls or treated with a topical ointment containing 7 mg anti-nfP2X$_7$ antibody/g ointment base. Treatments were applied on days 5, 9, 13 and 16. Tumour sizes were measured on day 5 after injection and subsequently every two days thereafter until day 19 at which time mice were killed. The results are shown in Figure 8. A statistically significant reduction in tumour growth is evident (P<0.0001) from the date of the second treatment i.e. within 4 days of the initial application of the antibody.

In vivo efficacy in a cat with untreatable SCC of the nose

Approval was sought by a specialist veterinary oncology group to test the antibody on a cat presenting with an otherwise advanced

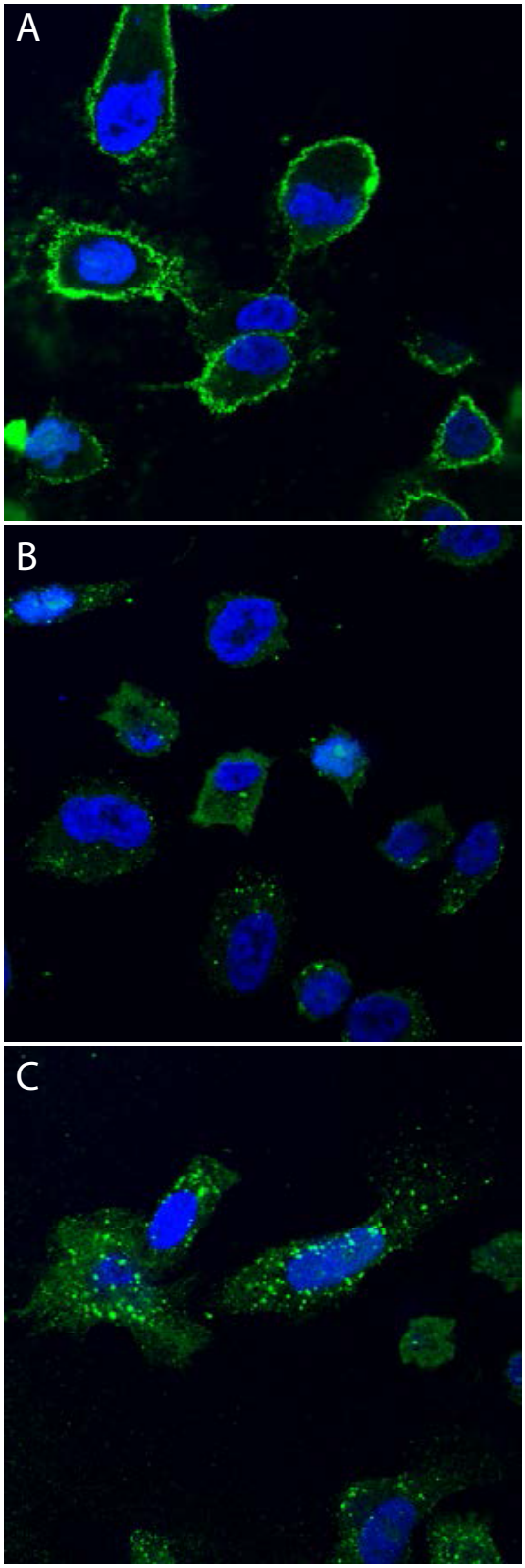

Figure 5: Internalisation of sheep anti nfP2X$_7$. PC3 cells on coverslips were preincubated on ice with 100 nM FITC conjugated affinity purified sheep anti-nfP2X$_7$ IgG antibody for 30 minutes. Coverslips were washed and then fixed immediately **(A)** or incubated at 37°C for 30 minutes **(B)** or 2 hours **(C)** before fixation. Representative images are shown. Fields of view 100 µm.

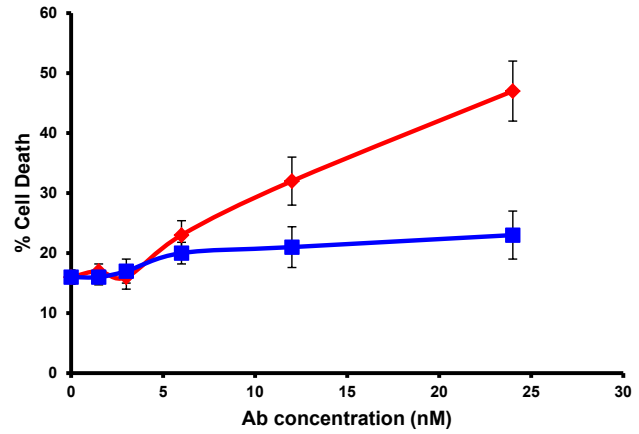

Figure 6: Killing of D270 human malignant glioma cells using a sub-optimal dose of cisplatin (15 μM) and either pre-immune control sheep antibody (blue) or specific sheep anti-nfP2X$_7$ IgG antibody (red) over the range 0-24 nM at 37°C after 24 h.

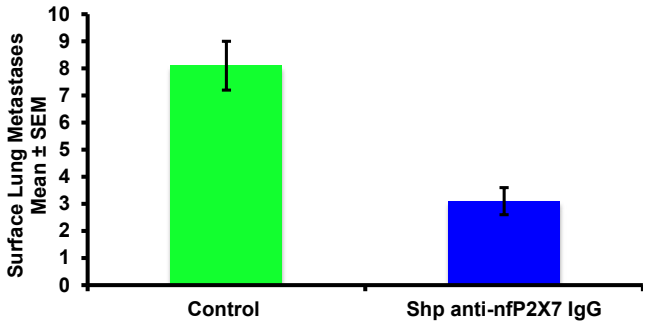

Figure 7: Inhibition of lung metastases spread from a subcutaneous implant of mouse breast tumour cells in Balb/C mice. Groups were injected with control buffer (green) and sheep anti-nfP2X$_7$ IgG at 10 mg/kg (blue). A statistically significant reduction in the number of lung metastases was measured between the treatment group and the control group (P<0.001).

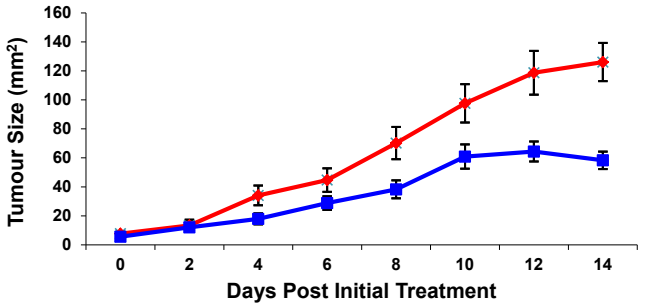

Figure 8: Inhibition of growth in mouse B16 melanoma cells injected intradermally and treated on Days 0, 4, 8 and 11 after a 5 day initial growth phase. Mice were sacrificed on Day 14. Untreated mice (red) showed significantly higher tumour growth than the group treated with specific antibody (blue).

squamous cell carcinoma originating in the left nostril but invading throughout the nasal cavity (bilaterally) and extending to the top of the left orbit and across each maxilla. Surgery was declined due to the invasiveness of the procedure and the low likelihood of complete excision. A biopsy was taken from the left nostril and stained for target receptor. Figure 9 shows that just like human cancer tissue and marsupial cancer tissue, feline SCC stained strongly and specifically for nfP2X$_7$. The surrounding normal tissue is completely devoid of target receptor and there is no cross-reactivity. Sterile antibody (dose 4 mg/kg or 20 mg for the 5 kg cat) was prepared for intravenous injection via a canula in the left cephalic vein and the solution diluted in sterile saline at 1.6 mg/mL and administered via a pump over 1 h. The patient tolerated the foreign antibody very well. Bloods were collected and no anomolies detected. Figure 10a shows the patient at the start of treatment. The patient returned for treatment on Day 7 (Figure 10b). The lesion had formed an eschar and began lifting from the nasal bridge. The dose was increased to 6 mg/kg as the first dose was so well tolerated. On Day 14 (Figure 10c) another 30 mg (6 mg/kg) was administered. The nasal scabbing was markedly resolved and the lesion had become pink

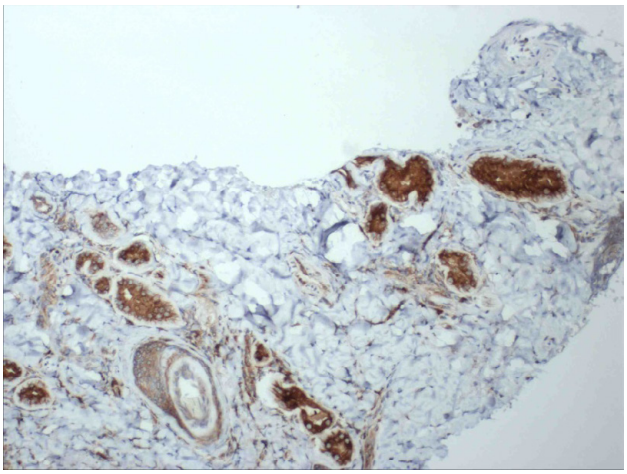

Figure 9: Immunohistochemistry staining for nfP2X$_7$ receptor expression in the biopsy of a cat with a deeply invasive nasal SCC. Note heavily stained cancer cells in islands distributed through the tissue. The lesion extended across the nose bilaterally extending to the left orbit, an area of up to 8 cm^2. Surgery was not indicated.

Figure 10: A feline nasal SCC before during and after treatment with 5 mg/kg affinity purified sterile sheep anti-nfP2X$_7$ antibody in a saline drip administered intravenously at 1 mg/mL over 1 h weekly for three weeks. Figure 10A shows the cat on the day of the initial treatment. The biopsy suture is visible on the left distal nostril. The underlying lesion extends across the entire nose and discolouration is apparent delineating the outline stretching to the upper left orbit and across each maxilla. Figure 10B is at Week 1, Figure 10C at Week 2 and Figure 10D at Week 3 by which stage no further treatment was given.

and alopecic. At Day 21 (Figure 10d), the benefits of the previous three doses were apparent. The lesion appeared completely resolved and new pink epithelialised tissue was present. Nevertheless, an additional 30 mg (6 mg/kg) treatment was administered on Day 21. An additional dose was administered a month later as a precaution against recurrence. The patient was re-examined with periodic follow-up over 2 years with no recurrence being detected. Blood samples were tested for the presence of anti-sheep antibody. By Week 4 the level of these antibodies was clear as demonstrated by ELISA.

Discussion

We previously showed that monoclonal antibodies developed for diagnostic detection of nfP2X$_7$ in FFPE human cancer tissues have shown high specificity across a wide range of human cancer types including but not limited to bowel, lung, breast, prostate, pancreatic, gastric, head and neck, skin, brain and Hodgkin's lymphoma [27]. The target epitope underlies the ATP binding sites. These ATP sites only form when the P2X$_7$ monomers are correctly packed in the assembled trimer inserted into the plasma membrane. These target binding sites for the specific antibody are sequence conserved across species as evidenced by the ability of the antibody developed against the human sequence to detect the exposed epitopes on nfP2X$_7$ receptors expressed on the surface of cancer cells from the marsupial Tasmanian Devil affected with facial tumour disease (Figure 1) both in the primary and in the metastatic cells spread to the lungs. The genotype and the karyotype of the cells extracted from DFTD tumours from different animals are consistent while being distinct from their hosts thus supporting the transmission of the disease between animals. This is a cancer of the Schwann cells that is rapidly depleting stocks of wild animals [31].

This conserved target indicates that the structure underlying and supporting the ATP site is critical to receptor function. While many differences have arisen in the sequence of the receptor between species, the target epitope has remained invariant. Any mutation that alters the ATP binding constant is potentially fatal given the low binding constant [26]. Such an invariant target exposed in receptors, unable to initiate the apoptotic signal on cells across many species, makes it ideal for development of specific therapeutics. Off-target binding of therapeutics developed in oncology give rise to unwanted side effects that can be costly through the need for increased doses to reach desired therapeutic concentrations and adverse effects on binding to non-cancer target tissue.

The nfP2X$_7$ receptor density appears to increase on the plasma membrane of affected cancer cells as their level of transformation increases. This is evident in prostate cancer tissue where normal tissue is seen to be devoid of receptor while well differentiated tumour tissue has only a moderate receptor density. As the tumour cells transform to moderately differentiated or poorly differentiated states, the density of receptors increases (Figure 2). Certainly, very slow growing low grade prostate cancers exhibit a pattern of receptor expression that is almost entirely intracellular, while cases of invasive prostate cancer exhibit more plasma membrane and basal cell labelling in advance of stromal invasion from the apical epithelium together with a significantly elevated cell surface receptor density [16,32,33].

The expression of P2X$_7$ receptor is regulated by DNA methylation. In cervical cancer cells, the level of DNA methylation at the cis inhibitory element was reported to be higher than in normal cells [34]. In mammals, as both the DNA methyltransferases and a number of the histone methyltransferases play a role in the maintenance of DNA methylation [35-37], inhibition of these enzymes may be one mechanism by which an increased expression of P2X$_7$ receptor occurs in cancers. Higher intratumoral expression has been found to be strongly correlated with poor patient outcome in clear-cell renal cell carcinoma [38]. Such mechanisms may facilitate the use of P2X$_7$ receptor as a potential target for the novel immunotherapeutic approach of treating cancers.

Besides the up-regulation of P2X$_7$ in prostate cancer observed by other groups [39], the receptor is expressed at high level in its non-functional form [15,40], an example of which involved the E496A mutant [41], a mutation found to produce a loss of pore functionality [42]. Additional confirmations, many very recently, of the up-regulation of the receptor in cancer tissue have been obtained for pancreatic [43], lung [44], skin [45-47], brain [48,49], renal [38], prostate [50], thyroid [51], bone [52] and both ALL and AML [53,54].

A previously developed monoclonal antibody raised against the same target was able to bind well to fixed tissue but was a poor binder against live cells. The affinity of the purified polyclonal antibody of type IgG raised in sheep was investigated for its ability to bind to the target expressed on live cells. Figures 3 and 4 show good specific binding of the antibody to both the expressed extracellular domain of the P2X$_7$ monomer that presents the exposed epitope that is otherwise hidden in the correctly packed trimer on normal tissue as well as an example of the strong binding to the exposed epitope on the trimer of nfP2X$_7$ as expressed on cancer cells, COLO205 being just an example. The control antibody showed only trivial binding. Similarly, the specific antibody does not bind to the membrane surface of tissue that is normal, a result reinforced in testing of the antibody in a panel of normal and cancer tissue as part of the toxicity component for the FDA trial (NCT02587819) conducted as part of a topical therapeutic trial against BCCs. In contrast, with clear binding to nfP2X$_7$ receptors expressed on cancer cells, incubating the primary antibody with normal cells expressing equivalent density of P2X$_7$, but in fully functional form, such as human B-lymphocytes, shows no binding.

Binding to target cancer cells was accompanied by cellular uptake (Figure 5). Short incubation times revealed punctate patches of surface receptor while longer exposure resulted in more widespread binding to surface receptors. Prolonged exposure to antibody for 30 minutes or more resulted in endocytosis of both receptor and bound antibody.

The therapeutic potential of the naked antibody was demonstrated in the associated cell killing assays, an example of which is shown in Figure 6 where the human glioma cancer cell line D270 was affected by specific antibody binding but not by the controls in 24 h. The xenograft 4T1 model of lung metastases in immunocompetent mice showed a statistically significant reduction in mean metastatic tumour number (Figure 7) at $P<0.001$. However, the inhibition of primary tumours implanted subcutaneously was much less effective. Examination of the antibody penetration in these tissues showed a lack of blood supply and consequent lack of penetration while the metastases were more accessible to the antibody (data not shown). Anti-antibody immune responses in these immunocompetent mice necessarily limits the time over which efficacy can be studied. A similar model in immunocompetent mice inoculated with the mouse B16 melanoma cell line showed that even topical applications were able to inhibit tumour growth by 50% over two weeks (Figure 8). In this situation, little or no immune reaction to the foreign antibody would act as a limit to duration of efficacy. An orthotopic tumour model or preferably a spontaneous tumour growth model in companion animals would provide more realistic settings to test nfP2X$_7$ antibody efficacy.

A treatment case study is presented of a cat that presented with a deeply invasive and extensive nasal SCC unable to be effectively treated with alternatives. The results obtained showed rapid lesion clearance via systemic delivery before the anti-sheep antibody response could render the treatment ineffective. No anaphylactic reaction was observed with the four infusions over 21 days that were all well tolerated. A final infusion administered a month later also had no adverse effects but the likelihood of this additional dose having been effective in the case of non-clearance would have been reduced due to the presence of anti-sheep antibodies. Importantly, complete clearance was obtained in the short available treatment window and no recurrence was seen over more than two years.

In a separate study, where hyperimmune sheep were used to produce cGMP anti-nfP2X$_7$ antibody, regular bleeds over several years showed no ill effects. There was no sign of neutropaenia even though lymphocytes have a high density of functional P2X$_7$ receptor. These data support the specificity of the antibody for nfP2X$_7$ receptor. Sheep organs examined after several years exposure showed no toxic effects of the treatment. Specificity for the epitope on cancer cells thus appears to be extremely high as the epitope is otherwise hidden in normal cells expressing fully functional P2X$_7$ with pore forming capability.

The monoclonal antibody [27] to nfP2X$_7$ receptor appears highly specific and does not obviously bind on the surface of cells expressing only normal P2X$_7$ receptor. This specificity augurs well for a human therapeutic lead that may well have clinical benefits across a wide range of cancer indications. The benefits are specific targeting, lower doses needed to target the tumour, and no unwanted side effects from off-target binding. That the target is highly conserved across species indicates that mutational drift in the target, as a result of therapeutic intervention, as is the case with easily mutable targets such as BCR-ABL, c-KIT and PDGFRA tyrosine kinases [53,54], is less likely to occur.

Acknowledgements

The authors wish to thank Drs. A. Kreiss and G. Woods from the Menzies Institute for Medical Research, University of Tasmania for original supply of Tasmanian devil facial tumour samples. JB, AGB and LCT note their continued association with Biosceptre.

References

1. Li GH, Lee EM, Blair D, Holding C, Poronnik P, et al. (2000) The distribution of P2X receptor clusters on individual neurons in sympathetic ganglia and their redistribution on agonist activation. J Biol Chem 275: 29107-29112.
2. Kukley M, Barden JA, Steinhäuser C, Jabs R (2001) Distribution of P2X receptors on astrocytes in juvenile rat hippocampus. Glia 36: 11-21.
3. Moore KH, Ray FR, Barden JA (2001) Loss of purinergic P2X3 and P2X5 receptor innervation in human detrusor from adults with urge incontinence. J Neurosci 21: 166.
4. Ray FR, Moore KH, Hansen MA, Barden JA (2003) Loss of purinergic P2X receptor innervation in human detrusor and subepithelium from adults with sensory urgency. Cell Tissue Res 314: 351-359.
5. Nagy PV, Fehér T, Morga S, Matkó J (2000) Apoptosis of murine thymocytes induced by extracellular ATP is dose- and cytosolic pH-dependent. Immunol Lett 72: 23-30.
6. Coutinho-Silva R, Persechini PM, Bisaggio RD, Perfettini JL, Neto AC, et al. (1999) P2Z/P2X7 receptor-dependent apoptosis of dendritic cells. Am J Physiol 276: C1139-1147.
7. Chused TM, Apasov S, Sitkovsky M (1996) Murine T lymphocytes modulate activity of an ATP-activated P2Z-type purinoceptor during differentiation. J Immunol 157: 1371-1380.
8. Di Virgilio F, Chiozzi P, Ferrari D, Falzoni S, Sanz JM, et al. (2001) Nucleotide receptors: an emerging family of regulatory molecules in blood cells. Blood 97: 587-600.
9. Humphreys BD, Rice J, Kertesy SB, Dubyak GR (2000) Stress activated protein kinase/JNK activation and apoptotic induction by the macrophage P2X7 nucleotide receptor. J Biol Chem 275: 26792-26798.
10. Grahames CB, Michel AD, Chessell IP, Humphrey PP (1999) Pharmacological characterization of ATP- and LPS-induced IL-1beta release in human monocytes. Br J Pharmacol 127: 1915-1921.
11. Gu BJ, Saunders BM, Petrou S, Wiley JS (2011) P2X7 is a scavenger receptor for apoptotic cells in the absence of its ligand, extracellular ATP. J Immunol 187: 2365-2375.
12. Gu BJ, Sun C, Fuller S, Skarratt KK, Petrou S, et al. (2014) A quantitative method for measuring innate phagocytosis by human monocytes using real-time flow cytometry. Cytometry A 85: 313-321.
13. Lovelace MD, Gu BJ, Eamegdool SS, Weible MW 2nd, Wiley JS, et al. (2015) P2X7 receptors mediate innate phagocytosis by human neural precursor cells and neuroblasts. Stem Cells 33: 526-541.
14. Slater M, Scolyer RA, Gidley-Baird A, Thompson JF, Barden JA (2003) Increased expression of apoptotic markers in melanoma. Melanoma Res 13: 137-145.
15. Slater M, Danieletto S, Pooley M, Teh LC, Gidley-Baird A, et al. (2004) Differentiation between cancerous and normal hyperplastic lobules in breast lesions. Breast Cancer Res Treat 83: 1-10.
16. Slater M, Danieletto S, Gidley-Baird A, Teh LC, Barden JA (2004) Early prostate cancer detected using expression of non-functional cytolytic P2X7 receptors. Histopathology 44: 206-216.
17. Garcia-Marcos M, Perez-Andres E, Tandel S, Fontanils U, Kumps A, et al. (2006) Coupling of two pools of P2X7 receptors to distinct intracellular signaling pathways in rat submandibular gland. J Lipid Res 47: 705-714.
18. Surprenant A, Rassendren F, Kawashima E, North RA, Buell G (1996) The cytolytic P2Z receptor for extracellular ATP identified as a P2X receptor (P2X7). Science 272: 735-738.
19. Rassendren F, Buell GN, Virginio C, Collo G, North RA, et al. (1997) The permeabilizing ATP receptor, P2X7. Cloning and expression of a human cDNA. J Biol Chem 272: 5482-5486.
20. Virginio C, MacKenzie A, Rassendren FA, North RA, Surprenant A (1999) Pore dilation of neuronal P2X receptor channels. Nat Neurosci 2: 315-321.
21. Worthington RA, Smart ML, Gu BJ, Williams DA, Petrou S, et al. (2002) Point mutations confer loss of ATP-induced human P2X(7) receptor function. FEBS Lett 512: 43-46.
22. Samways DS, Khakh BS, Dutertre S, Egan TM (2011) Preferential use of unobstructed lateral portals as the access route to the pore of human ATP-gated ion channels (P2X receptors). Proc Natl Acad Sci U S A 108: 13800-13805.
23. Gu BJ, Field J, Dutertre S, Ou A, Kilpatrick TJ, et al. (2015) A rare P2X7 variant Arg307Gln with absent pore formation function protects against neuroinflammation in multiple sclerosis. Hum Mol Genet 24: 5644-5654.
24. Virginio C, MacKenzie A, North RA, Surprenant A (1999) Kinetics of cell lysis, dye uptake and permeability changes in cells expressing the rat P2X7 receptor. J Physiol 519 Pt 2: 335-346.
25. Morelli A, Chiozzi P, Chiesa A, Ferrari D, Sanz JM, et al. (2003) Extracellular ATP causes ROCK I-dependent bleb formation in P2X7-transfected HEK293 cells. Mol Biol Cell 14: 2655-2664.
26. Barden JA, Sluyter R, Gu BJ, Wiley JS (2003) Specific detection of non-functional human P2X(7) receptors in HEK293 cells and B-lymphocytes. FEBS Lett 538: 159-162.
27. Barden JA, Yuksel A, Pedersen J, Danieletto S, Delprado W (2014) Non-functional P2X7: A novel and ubiquitous target in human cancer. J Clin Cell Immunol 5: 237-241.
28. Jelassi B, Chantome A, Alcaraz-Perez F, Baroja-Mazo A, Cayuela ML, et al. (2011) P2X7 receptor activation enhances SK3 channels and cysteine cathepsin-dependent cancer cells invasiveness. Oncogene 30: 2108-2122.
29. Sluyter R, Stokes L (2011) Significance of P2X7 receptor variants to human health and disease. Recent Pat DNA Gene Seq 5: 41-54.
30. Knight MJ, Riffkin CD, Ekert PG, Ashley DM, Hawkins CJ (2004) Caspase-8

levels affect necessity for mitochondrial amplification in death ligand-induced glioma cell apoptosis. Molec. Carcinogen 39: 173-82.

31. Murchison EP, Tovar C, Hsu A, Bender HS, Kheradpour P, et al. (2010) The Tasmanian devil transcriptome reveals Schwann cell origins of a clonally transmissible cancer. Science 327: 84-87.

32. Maianski Z, Pedersen J, Chabert C, Barden JA, Stricker PD (2007) Evaluation of a new monoclonal antibody targeting the apoptotic purinergic receptor P2X7, as a diagnostic tool for prostate cancer. Journal of Urol 177: 474.

33. Barden JA, Gidley-Baird A, Armstrong A, Bean P, Pilkington G, et al. (2009) Evaluation of non-functional P2X7 receptor as a potential pan cancer therapeutic and diagnostic target. Cancer Res 69: 153.

34. Zhou L, Luo L, Qi X, Li X, Gorodeski GI (2009) Regulation of P2X(7) gene transcription. Purinergic Signal 5: 409-426.

35. Bestor T, Laudano A, Mattaliano R, Ingram V (1988) Cloning and sequencing of a cDNA encoding DNA methyltransferase of mouse cells. The carboxyl-terminal domain of the mammalian enzymes is related to bacterial restriction methyltransferases. J Mol Biol 203: 971-983.

36. Okano M, Bell DW, Haber DA, Li E (1999) DNA methyltransferases Dnmt3a and Dnmt3b are essential for de novo methylation and mammalian development. Cell 99: 247-257.

37. Zhang T, Termanis A, Özkan B, Bao XX, Culley J, et al. (2016) G9a/GLP Complex Maintains Imprinted DNA Methylation in Embryonic Stem Cells. Cell Rep 15: 77-85.

38. Liu Z, Liu Y, Xu L, An H, Chang Y, et al. (2015) P2X7 receptor predicts postoperative cancer-specific survival of patients with clear-cell renal cell carcinoma. Cancer Sci 106: 1224-1231.

39. Ravenna L, Sale P, Di Vito M, Russo A, Salvatori L, et al. (2009) Up-regulation of the inflammatory-reparative phenotype in human prostate carcinoma. Prostate 69: 1245-1255.

40. Slater M, Danieletto S, Barden JA (2005) Expression of the apoptotic calcium channel P2X7 in the glandular epithelium. J Mol Histol 36: 159-165.

41. Ghalali A, Wiklund F, Zheng H, Stenius U, Högberg J (2014) Atorvastatin prevents ATP-driven invasiveness via P2X7 and EHBP1 signaling in PTEN-expressing prostate cancer cells. Carcinogenesis 35: 1547-1555.

42. Gu BJ, Zhang W, Worthington RA, Sluyter R, Dao-Ung P, et al. (2001) A Glu-496 to Ala polymorphism leads to loss of function of the human P2X7 receptor. J Biol Chem 276: 11135-11142.

43. Künzli BM, Berberat PO, Giese T, Csizmadia E, Kaczmarek E, et al. (2007) Upregulation of CD39/NTPDases and P2 receptors in human pancreatic disease. Am. J. Physiol. Gastrointest. Liver Physiol 29: G223-230.

44. Schmid S, Kübler M, Korcan Ayata C, Lazar Z, Haager B, et al. (2015) Altered purinergic signalling in the tumor associated immunologic microenvironment in metastasized non-small-cell lung cancer. Lung Cancer 90: 516-521.

45. Greig AV, Linge C, Healy V, Lim P, Clayton E, et al. (2003) Expression of purinergic receptors in non-melanoma skin cancers and their functional roles in A431 cells. J Invest Dermatol 1: 315-327.

46. Slater M, Barden JA (2005) Differentiating keratoacanthoma from squamous cell carcinoma by the use of apoptotic and cell adhesion markers. Histopathology 47: 170-178.

47. White N, Butler PE, Burnstock G (2005) Human melanomas express functional P2 X(7) receptors. Cell Tissue Res 321: 411-418.

48. Raffaghello L, Chiozzi P, Falzoni S, Di Virgilio F, Pistoia V (2006) The P2X7 receptor sustains the growth of human neuroblastoma cells through a substance P-dependent mechanism. Cancer Res 66: 907-914.

49. Amoroso F, Capece M, Rotondo A, Cangelosi D, Ferracin M, et al. (2015) The P2X7 receptor is a key modulator of the PI3K/GSK3beta/VEGF signaling network: evidence in experimental neuroblastoma. Oncogene 34: 5240-5521.

50. Qiu Y, Li WH, Zhang HQ, Liu Y, Tian XX, et al. (2014) P2X7 mediates ATP-driven invasiveness in prostate cancer cells. PLoS One 9: e114371.

51. Solini A, Cuccato S, Ferrari D, Santini E, Gulinelli S, et al. (2008) Increased P2X7 receptor expression and function in thyroid papillary cancer: a new potential marker of the disease? Endocrinology 149: 389-396.

52. Adinolfi E, Amoroso F, Giuliani AL (2012) P2X7 Receptor Function in Bone-Related Cancer. J Osteoporos 2012: 637863.

53. Milojkovic D, Apperley J (2009) Mechanisms of Resistance to Imatinib and Second-Generation Tyrosine Inhibitors in Chronic Myeloid Leukemia. Clin Cancer Res 15: 7519-7527.

54. Bixby D, Talpaz M (2011) Seeking the causes and solutions to imatinib-resistance in chronic myeloid leukemia. Leukemia 25: 7-22.

Citation: Barden JA, Gidley-Baird A, Teh LC, Rajasekariah GH, Pedersen J, et al. (2016) Therapeutic Targeting of the Cancer-Specific Cell Surface Biomarker nfP2X$_7$. J Clin Cell Immunol 7: 432. doi:10.4172/2155-9899.1000432